

Supplementary information for:

PRECISION MARANGONI-DRIVEN PATTERNING

Talha A. Arshad,^{a,b} Chae Bin Kim,^a Nathan A. Prisco,^a Joshua M. Katzenstein,^a Dustin W.

Janes,^a Roger T. Bonnecaze,^{a,b,c} and Christopher J. Ellison^{a,c}*

^aMcKetta Department of Chemical Engineering, ^bNanomanufacturing Systems for Mobile Computing and Mobile Energy Technologies (NASCENT) Center, and ^cTexas Materials Institute, The University of Texas at Austin, 200 East Dean Keeton Street, Austin, Texas 78712, United States

Supporting Information Table of Contents

I:	Initial Concentration Profile.....	(pg. S2)
II:	Glass Transition Temperature of PS	(pg. S3)
III:	Viscosity of PS blend at 120 °C	(pg. S5)
IV:	Extracting Surface Tension and Diffusivity.....	(pg. S5)
V:	Secondary Peaks at Short Thermal Annealing.....	(pg. S7)

I: Initial Concentration Profile

For fluorescence microscopy experiments, a nitrobenzofurazan (NBD) fluorophore attached to polystyrene (PS) was synthesized as described earlier.¹ Toluene or cyclopentanone solutions containing NBD-labeled PS ($M_n = 2900$ g/mol, $\bar{D} = 1.2$) and dye-unlabeled PS possessing identical molecular weight were spin coated onto quartz substrates. To prevent fluorophore self-quenching, the amount of fluorophore content was limited to 0.18 wt. % of the total dry film mass.² The UV exposure dose typically used for patterning, 840 J/cm², was applied to the films through a line-and-space photo-mask possessing 25 μm pattern periodicity. The fluorescence intensity profile after photobleaching the NBD dye was obtained by imaging with a Hamamatsu Orca R2 camera with $\mu\text{Manager}$ software for camera control³ on an Olympus BX 51 epifluorescence microscope coupled to a Photon Technologies Quanta Master 40 fluorimeter. The excitation wavelength used was 465 nm with a 4 nm bandpass and an emission filter selected for all wavelengths greater than 520 nm. Because the NBD-labeled PS content has been set below the threshold for self-quenching, this intensity is linearly proportional to the concentration of NBD. The depth of focus of the microscope is 2.9 μm , which is much larger than the typical thicknesses of films used in this study; therefore, fluorescence of the film is captured from the entire depth. Informed by the NBD concentration profile of the bleached NBD-labeled PS after light exposure through the mask, a smoothed step function was used to generate the initial concentration profile for simulations. For one half-period of the mask pattern, this is given by:

$$\frac{c}{c_0}\left(\frac{x}{\lambda}, t = 0\right) = 6\left(\frac{x}{\lambda}\right)^5 - 15\left(\frac{x}{\lambda}\right)^4 + 10\left(\frac{x}{\lambda}\right)^3 \quad (1)$$

The fluorescence intensity profile as well as the initial concentration profile employed in simulations is shown in Figure S1.

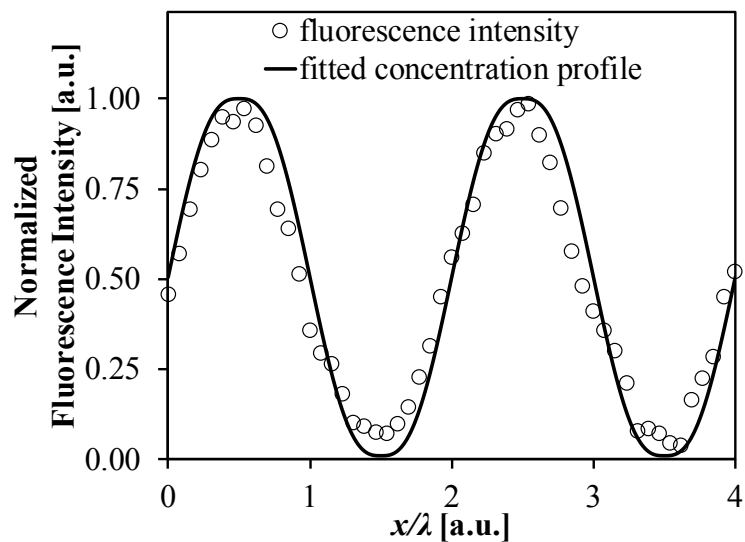


Figure S1: Normalized fluorescence intensity profile obtained experimentally from fluorescence microscopy using NBD labeled PS after typical exposure protocol for patterning was performed. Solid line represents the initial concentration profile used in the model prediction.

II: Glass Transition Temperature of PS

The glass transition temperature, T_g , of the atactic PS used in this study was determined by differential scanning calorimetry (DSC) using a Mettler-Toledo DSC-1. The sample was heated to 150 °C at a rate of 20 °C/min for the first 2 cycles then was heated to 300 °C at 15 °C/min for the last 2 cycles. All of the heating thermograms show no T_g shifts between each cycle. The DSC thermogram shown in Figure S2 corresponds the last heating step up to 300 °C which shows the PS possesses a bulk T_g of 61 °C.

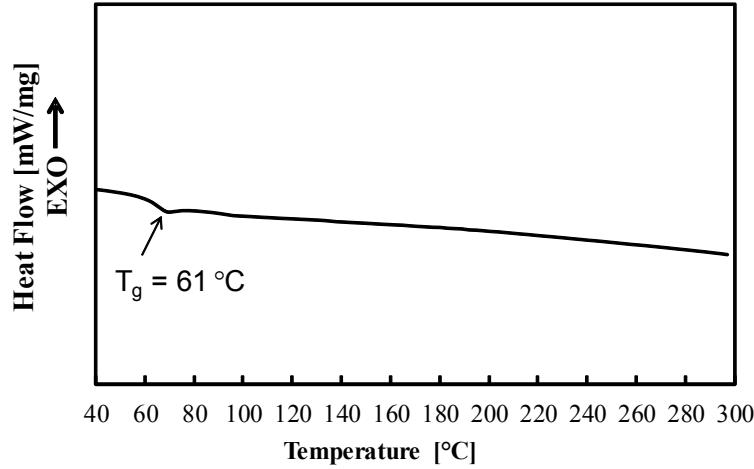


Figure S2. DSC thermogram of PS taken upon heating at a rate of 15 °C/min to 300 °C.

The glass transition temperature, T_g , of a thin PS film before and after a typical patterning light exposure procedure was determined by spectroscopic ellipsometry. The results are shown in Figure S2. The film was heated at 120 °C for 5 min, and then cooled at 2 °C/min to -20 °C. The film's thickness, $h(T)$, was determined at each sample temperature, T , using a layered model that fitted the optical constants and film thickness. The T_g was found by regressing the equation⁴

$$h(T) = w \left(\frac{M - G}{2} \right) \ln \left[\cosh \left(\frac{T - T_g}{w} \right) \right] + (T - T_g) \left(\frac{M + G}{2} \right) + c \quad (2)$$

to the data. . The parameters M , G , T_g , and c were fitted and the glass transition width was set as $w = 10$ °C. Using larger or smaller values of w did not change the extracted value of T_g more than 1 °C.

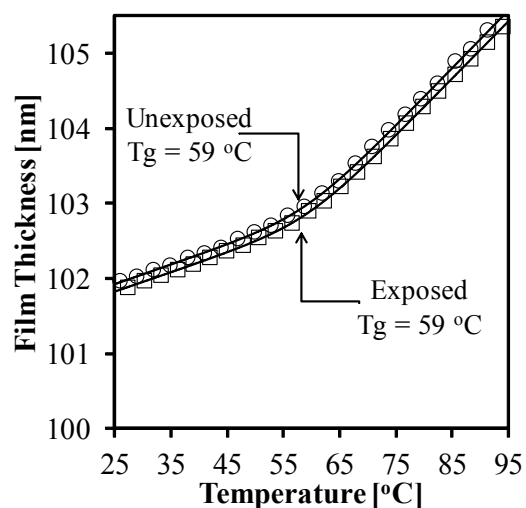


Figure S3. Effect of blanket exposure to 140 J/cm² of broadband light on the glass transition of a PS film on Si substrate as determined by spectroscopic ellipsometry. For clarity only every 100th data point is displayed. The solid lines represent regressions of Eq. 2 to the data.

III: Viscosity of PS blend at 120 °C

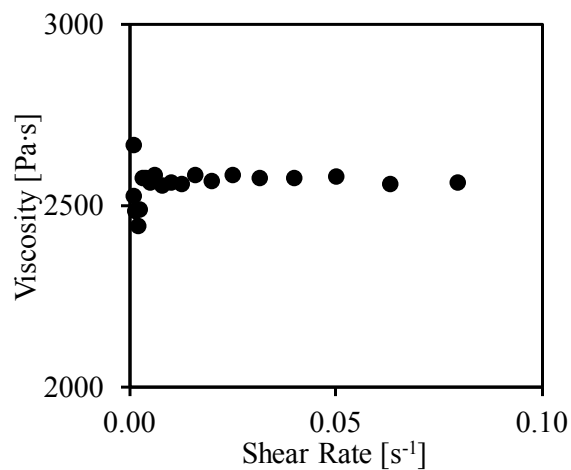


Figure S4: Viscosity of the polystyrene blend (99 wt.% $M_n = 2.9$ kDa PS, 1 wt.% $M_n = 50$ kDa PS) was measured at 120 °C using a TA Instruments AR-2000ex rheometer under steady shear.

IV: Extracting Surface Tension Gradients and Diffusivities

The linearized solution gives, for the peak to valley height in dimensionless form:

$$\hat{\eta} = \frac{\pi^2 \frac{\Delta\gamma c_0}{2}}{\psi_1 - \psi_2} (e^{\psi_1 t} - e^{\psi_2 t}) \quad (3)$$

Substituting in the Taylor series expansion for the exponential function and retaining terms only up to first order yields the evolution of peak-to-valley height at short times:

$$\hat{\eta} \approx \left(\pi^2 \frac{\Delta\gamma c_0}{2} \right) t \quad \forall \quad t \ll 1 \quad (4)$$

Comparing this to short-time experimental results, the difference in surface tension between the exposed and unexposed polymer ($\Delta\gamma$) can be extracted from the slope of the line.

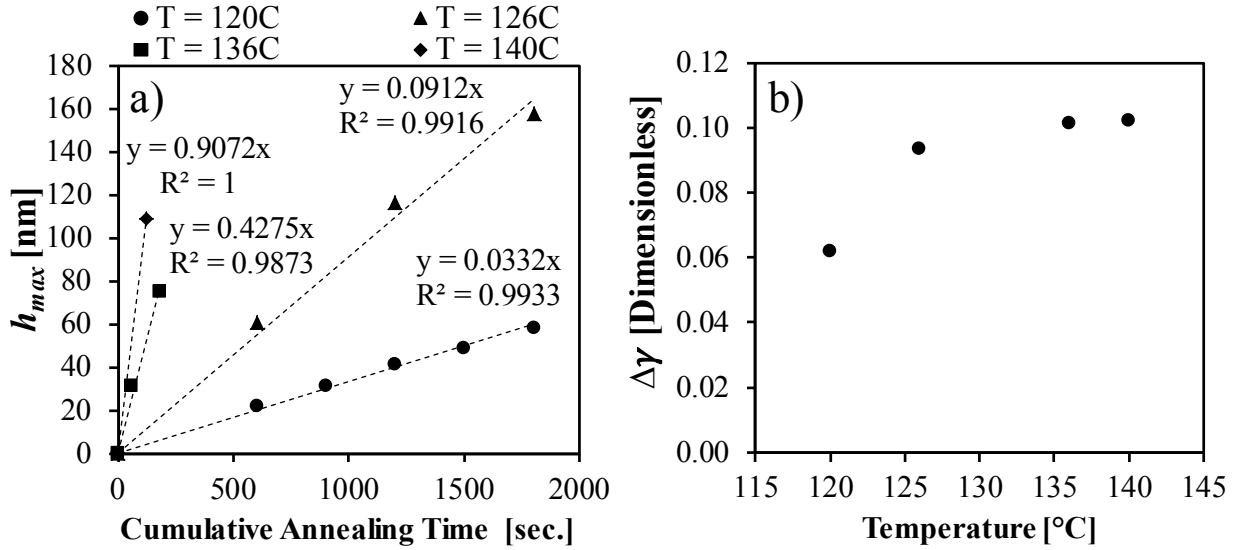


Figure S5: (a) Experimental results at short times (b) Non-dimensional surface tension difference values extracted from experimental data at four different temperatures.

At long times, peak-to-valley height reduces to

$$\hat{\eta} \approx \frac{\pi^2 \frac{\Delta\gamma c_0}{2}}{|\psi_1 - \psi_2|} e^{\psi_{max} t} \quad \forall \quad t \gg 1 \quad (5)$$

where $\psi_{max} \equiv \max_{x \in [0,1]}(\psi_1, \psi_2)$. This can be re-written as

$$\ln(\hat{\eta}) \approx \ln\left(\frac{\pi^2 \frac{\Delta\gamma c_0}{2}}{|\psi_1 - \psi_2|}\right) + (\psi_{max})t \quad (6)$$

Since the eigenvalues ψ_1 and ψ_2 are a function of diffusivity, it can be extracted by comparing this expression with experimental observations for peak-to-valley height at long times. As noted in the main text, the linearized solution is valid for cases where the features are small compared to the thickness of the unperturbed film. This is always true at short times, but applies at long times only for low temperatures or small initial conversions. For this reason diffusivity was extracted using experimental results at 120 °C and extrapolated to higher temperatures using correlations from literature (after shifting them to agree with the extrapolated value).

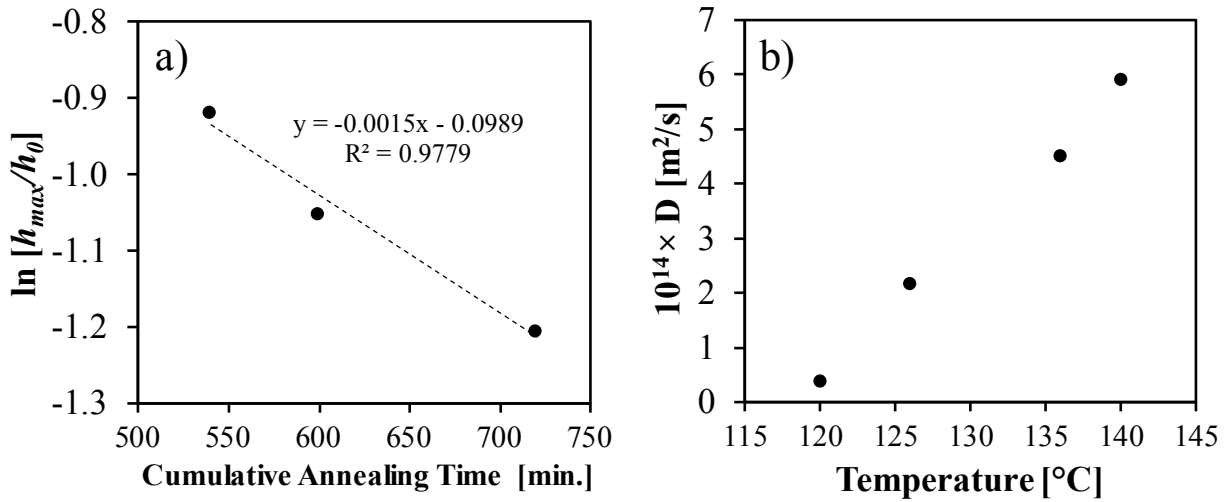


Figure S6: (a) Experimental results at 120°C for long times (b) Diffusivity values extracted from experimental data at 120°C and extrapolated to higher temperatures as in Ref. 5.

V: Secondary Peaks at Short Times

Simulations show that secondary peaks always form when a surface tension profile is present (see **Results** section in main paper), but their longevity varies. When the mask periodicity is relatively small, short annealing times are necessary to observe them experimentally.

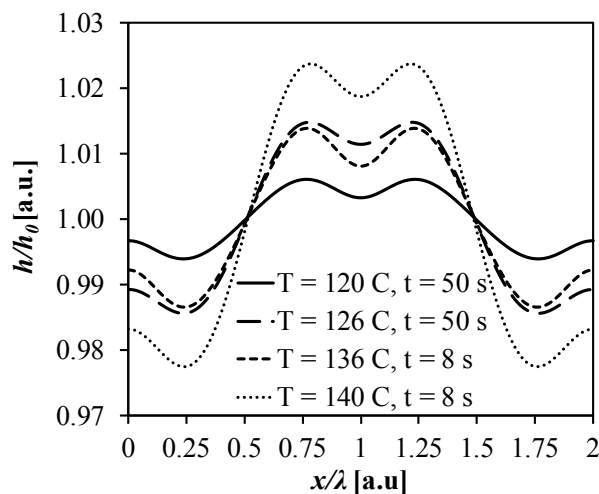


Figure S7: Simulated film height profiles at short times clearly depict secondary peaks at four different annealing temperatures. Thicknesses of the film at each annealing temperature are identical to those used in Figure 3 of the main manuscript.

References

1. Katzenstein, J. M.; Janes, D. W.; Cushen, J. D.; Hira, N. B.; McGuffin, D. L.; Prisco, N. A.; Ellison, C. J. *ACS Macro Lett.* 2012, **1**, 1150-1154.
2. Katzenstein, J. M.; Janes, D. W.; Hocker, H. E.; Chandler, J. K.; Ellison, C. J. *Macromolecules* **2012**, *45*, 1544-1552.
3. Edelstein, A.; Amodaj, N.; Hoover, K.; Vale, R.; Stuurman, N. *Computer Control of Microscopes Using μ Manager*; John Wiley & Sons, Inc., 2001.
4. Dalnoki-Veress, K.; Forrest, J. A.; Murray, C.; Gigault, C.; Dutcher, J. R. *Phys. Rev. E* **2001**, *63*, 031801.
5. Fleischer, G. *Polym. Bull.* 1984, **11**, 75-80.